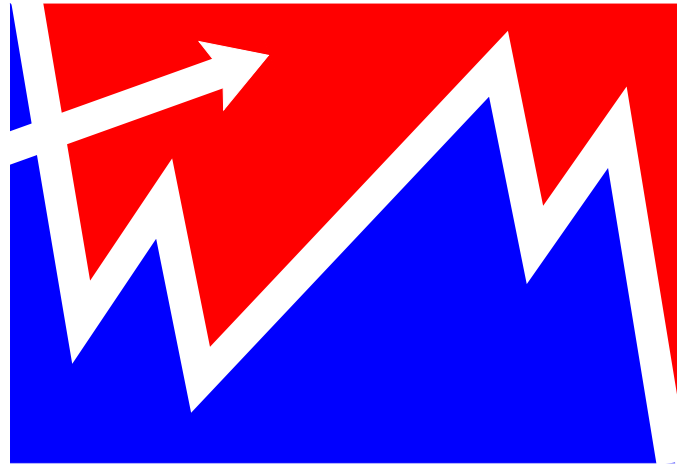


Quantum computation in presence of imperfections



QUANTWARE MIPS CENTER
CNRS, Université Paul Sabatier, Toulouse, France
<http://www.quantware.ups-tlse.fr/>

S.Bettelli, A.Chepelianskii, B.Georgeot, J.W.Lee,
B.Lévi, A.Pomeransky, M.Terraneo,
D.L.Shepelyansky (PI)

Supported by :
ARO/NSA/ARDA grant
EC RTN contract QTRANS
EC IST-FET project EDIQIP

Quantum computation of the Anderson transition in presence of imperfections

The stationary Schrödinger equation for the Anderson model: a particle on a d -dimensional lattice in a random potential:

$$\sum_{\vec{m}} V_{\vec{m}} \psi_{\vec{m}+\vec{n}} + E_{\vec{n}} \psi_{\vec{n}} = E \psi_{\vec{n}},$$

In $d \geq 3$ dimensions the wave functions are exponentially localized for sufficiently large (compared to $V_{\vec{m}}$) typical value of $E_{\vec{n}}$ and delocalized for small typical value of $E_{\vec{n}}$ (P.W. Anderson (1958)).

Our model: 1-dim. kicked rotator with frequency modulation. Anderson localization \rightarrow dynamical localization of quantum chaos in the kicked rotator model (S. Fishman et al. (1982)). 3 dimensions \rightarrow 1 dimension plus frequency modulation with 2 incommensurate frequencies. (D.L. Shepelyansky (1983)).

Our Hamiltonian H :

$$H_0(n) + k(1 + \epsilon \cos(\Omega_1 t) \cos(\Omega_2 t)) \cos \theta \sum_m \delta(t - m),$$

The time evolution:

$$\bar{\psi} = U_T U_k \psi, \quad U_T = \exp \{-iH_0(n)\}$$

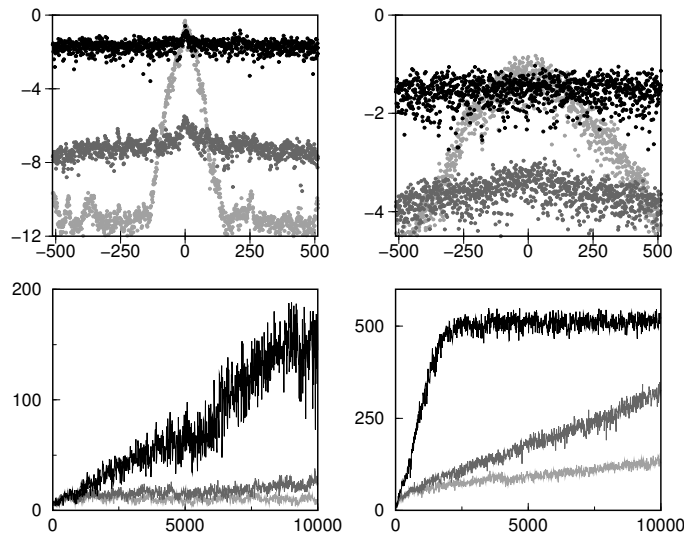
$$U_k = \exp \{-ik(1 + 0.75 \cos(\Omega_1 t) \cos(\Omega_2 t)) \cos \theta\}.$$

The quantum algorithm

The quantum states $n = 0, \dots, N - 1$ are represented by one quantum register with n_q qubits so that $N = 2^{n_q}$. The initial state with all probability at $n_0 = 0$ corresponds to the state $|00\dots 0\rangle$ (momentum n changes on a circle with N levels). The random phase multiplication $U_T = \exp(-iH_0(n))$ in the momentum basis is performed as a random sequence of one-qubit phase shifts and controlled-NOT gates. Then the kick operator $U_k = \exp(-ik(t) \cos \theta)$ is performed as follows. First, one applies the QFT to change the representation. Then θ can be written in the binary representation as $\theta/2\pi = 0.a_1a_2\dots a_{n_q}$ with $a_i = 0$ or 1. It's convenient to use the notation $\theta = \pi a_1 + \bar{\theta}$ to single out the most significant qubit. Then due to the relation $\cos \theta = (-1)^{a_1} \cos \bar{\theta} = \sigma_1^z \cos \bar{\theta}$ the kick operator takes the form $U_k = e^{-ik(t) \cos \theta} = e^{-i\sigma_1^z k(t) \cos \bar{\theta}}$. This operator can be approximated to an arbitrary precision by a sequence of one-qubit gates applied to the first qubit and the diagonal operators $S^m = e^{ima_1\bar{\theta}}$. We used the following sequence: $R_\gamma(\bar{\theta}) = HS^1H e^{-i\frac{\gamma}{4}\sigma_1^z} HS^{-2}H e^{-i\frac{\gamma}{2}\sigma_1^z} HS^2H e^{-i\frac{\gamma}{4}\sigma_1^z} HS^{-1}H = e^{-i\sigma_1^z \gamma \cos(\bar{\theta})} + O(\gamma^3)$, where $H = (\sigma_1^z + \sigma_1^x)/\sqrt{2}$ is the Hadamard gate. Thus the kick operator is given by $U_k = R_\gamma(\bar{\theta})^l + O(l\gamma^3)$, where the number of steps $l = k/\gamma$ and we used in our numerical simulations the small parameter $\gamma = k/l \approx 0.2$ that gives $l \approx 5 - 10$ for $k \sim 1 - 2$. The number of gates is $\sim k$, so the algorithm is more efficient for moderate k . Then one goes back to the momentum representation by the QFT. One complete iteration of the algorithm requires n_g elementary gates where $n_g = 2[k/\gamma](n_q + 2) + n_q^2 + 12n_q + 9$ with the square brackets denoting the integer part.

Effects of static imperfections

The model of static imperfections was introduced by B.Georgeot and D.Shepelyansky (1999). In this model all gates are perfect but between the gates acts a perturbation with Hamiltonian $\hat{\varphi} = \sum_j (\eta_j \sigma_j^z + \mu_j \sigma_j^x \sigma_{j+1}^x)$. Here η_j, μ_j vary randomly with $j = 1, \dots, n_q$.

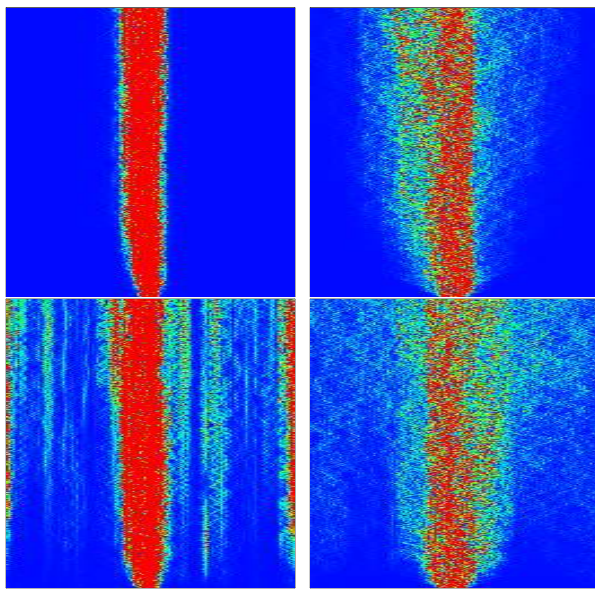


Top row: logarithm of probability $\log_{10} |\psi_n|^2$ vs. momentum n after $t = 10000$ iterations; dark gray curves are shifted down by 5 (left) and 2 (right). Bottom row: dependence of IPR ξ on time t . The left/right column corresponds to localized/delocalized phase at $k = 1.2$ and $k = 2.4$ respectively. The three curves represent $\epsilon = 0; 2 \times 10^{-5}; 6 \times 10^{-5}$ with color changing from light gray to black with increase of ϵ ; $\mu = \epsilon, n_q = 10$.

The Inverse Participation Ratio ξ is the inverse sum of the squares of the probabilities, $1/\xi = \sum_i |\psi_i|^4$, where $\xi \sim$ is the "number of nonzero components".

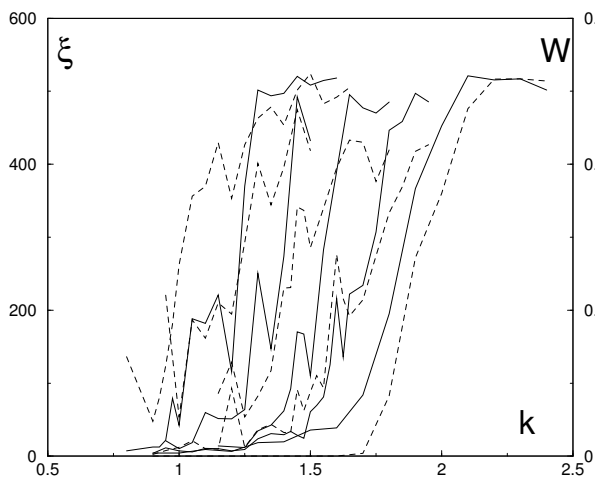
Static imperfections in QA for Anderson transition

The time evolution of the probability distribution $|\psi_n|^2$ in the localized (left column, $k = 1.2$) and delocalized (right column, $k = 2.4$) phases for



$n_q = 7$ qubits ($N = 2^{n_q}$), with $0 \leq t \leq 400$ (vertical axis) and $-N/2 < n \leq N/2$ (horizontal axis); $k_c = 1.8$. The strength of static imperfections is $\epsilon = \mu = 0$ for top row and $\epsilon = \mu = 10^{-4}$ for bottom row.

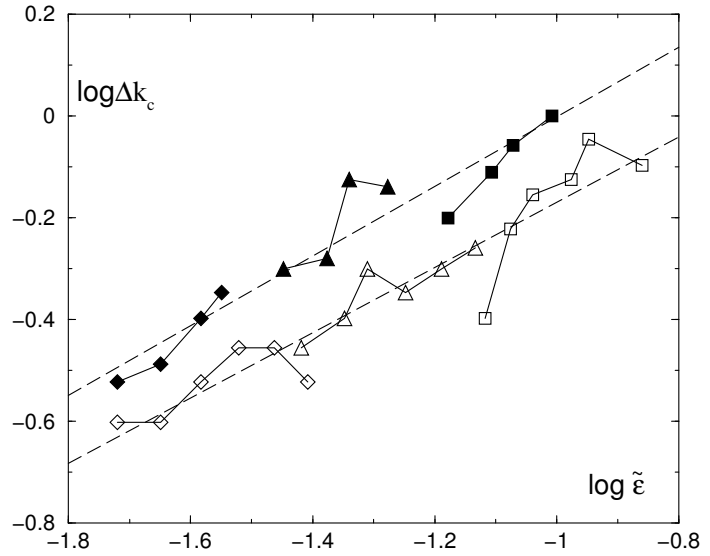
Dependence of the IPR ξ and the excitation probability:



$W = \sum_{n=(N/4, 3N/4)} |\psi_n|^2$ (full and dashed curves for left and right scales respectively) on the kick strength k for $n_q = 10$ and $t \geq 10^5$, $\epsilon = 0$; 10^{-5} ; 2×10^{-5} ; 4×10^{-5} ; 8×10^{-5} (curves from right to left); $\mu = 0$.

Critical point shift

Dependence of the shift of the critical point $\Delta k_c(\epsilon) = k_c - k_c(\epsilon)$ on rescaled imperfection strength $\tilde{\epsilon} = \epsilon n_g \sqrt{n_q}$ for $\epsilon = 2 \times 10^{-5}$ (diamonds), 4×10^{-5} (triangles) and 8×10^{-5} (squares); open/full symbols are for $\mu = 0$, $8 \leq n_q \leq 13$ and $\mu = \epsilon$, $8 \leq n_q \leq 11$ respectively; $k_c = 1.8$. The dashed lines show the scaling relation.



The shift of the critical point $\Delta k_c(\epsilon) = k_c - k_c(\epsilon)$ depends on ϵ , μ and n_q . From the IPR data obtained for various ϵ , μ , n_q we find that the global parameter dependence can be described by the scaling relation $\Delta k_c(\epsilon) = A\tilde{\epsilon}^\alpha$, $\tilde{\epsilon} = \epsilon n_g \sqrt{n_q}$. The data fit gives $A = 3.0$, $\alpha = 0.64$ for $\mu = 0$ and $A = 4.8$, $\alpha = 0.68$ for $\mu = \epsilon$.

In the vicinity of the critical point the algorithm gives a quadratic speedup in computation of diffusion rate and localization length, comparing to the known classical algorithms.

Imperfection effects for multiple applications of the quantum wavelet transform,
Phys. Rev. Lett. **90**, 257902 (2003)

Imperfection effects for multiple applications of the quantum wavelet transform

Wavelet Transforms (WT)

- Wavelets obtained by dilations and translations of an original **mother function**
- Frequency-time analysis
- Continuous and discrete WT.

Applications

- signal treatment - analysis and denoising of time series
- data and image compression
- multifractal analysis

Efficient implementation on Quantum Computers:
Daubeschies and Haar wavelet transforms

Circuit developed in *A. Fijaney and C. Williams, Lecture Notes in Computer Science* **1509**, 10 (Springer, 1998); *quant-ph/9809004*

QUANTUM ALGORITHM: the Daubechies wavelets

$$D^{(4)} = (D_4^{(4)} \oplus I_{2^{nq-4}})(\Pi_8 \oplus I_{2^{nq-8}}) \dots (D_{2^i}^{(4)} \oplus I_{2^{nq-2^i}})(\Pi_{2^{i+1}} \oplus I_{2^{nq-2^{i+1}}}) \dots \Pi_{2^{nq}} D_{2^{nq}}^{(4)}$$

- $D_{2^n}^{(4)}$ is the **wavelet kernel**, acting on vectors of length 2^n

$$D_{2^n}^{(4)} = (I_{2^{n-1}} \otimes C_1) P_{2^n} (N \otimes I_{2^{n-1}}) (N \otimes I_{2^{n-2}} \oplus I_{2^{n-1}}) \dots (N \otimes I_2 \oplus I_{2^{n-4}}) (N \oplus I_{2^{n-2}}) P_{2^n} (I_{2^{n-1}} \otimes C_0)$$

- P_{2^n} : permutation matrix, $P_{2^n} |a_0, a_1, \dots, a_{n-1}\rangle = |a_{n-1}, \dots, a_1, a_0\rangle$
- Π_{2^n} : shuffling matrix, $\Pi_{2^n} |a_0, a_1, \dots, a_{n-2}, a_{n-1}\rangle = |a_{n-1}, a_0, a_1, \dots, a_{n-2}\rangle$

N not gate - C_0, C_1 2×2 matrices related to the Daubechies coefficients

$$\tilde{C}_0 = 2 \begin{pmatrix} c_2 & c_3 \\ c_3 & -c_2 \end{pmatrix} \quad \tilde{C}_1 = \frac{1}{2} \begin{pmatrix} \frac{c_0}{c_3} & 1 \\ 1 & -\frac{c_0}{c_3} \end{pmatrix}$$

$$C_0 = \frac{1}{\sqrt{\det \tilde{C}_0}} \tilde{C}_0 \quad C_1 = \frac{1}{\sqrt{\det \tilde{C}_1}} \tilde{C}_1$$

Imperfection effects for multiple applications of the quantum wavelet transform,
 Phys. Rev. Lett. **90**, 257902 (2003)

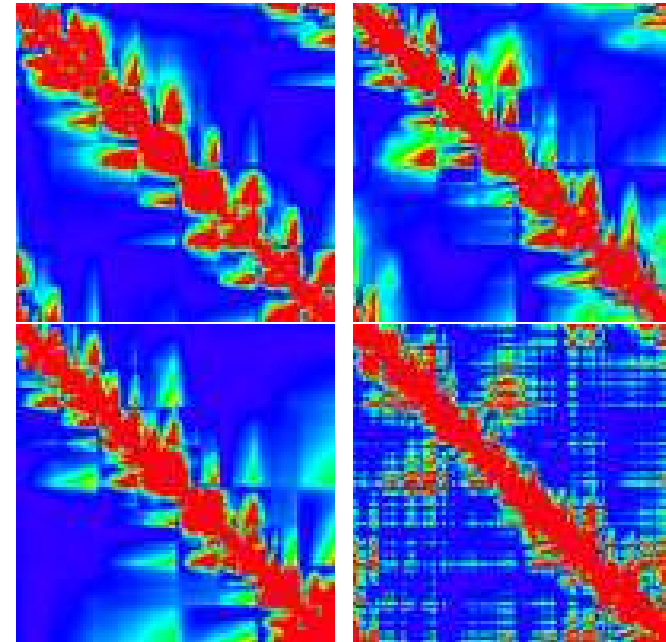
The Model

Dynamical model given by repeated applications of WT - efficient simulation on quantum computers. ψ in a Hilbert space of $N = 2^{n_q}$ states - dynamics described by the evolution operator \hat{U} :
 $\overline{\psi} = \hat{U}\psi$.

$$\hat{U} = D^{(4)\dagger} e^{-ik(x-\pi)^2/2} D^{(4)} e^{-iTn^2/2}$$

n momentum $-N/2 \leq n < N/2$, $x = 2\pi j/N$ with $j = 0, \dots, N-1$ index in the wavelet basis.

Algebraic localization: $|U_{n,n'}|^2 \sim \frac{1}{|n-n'|^\alpha}$
 $|n-n'| \gg 5k, \alpha = 4; |n-n'| \ll 5k, \alpha = 2$



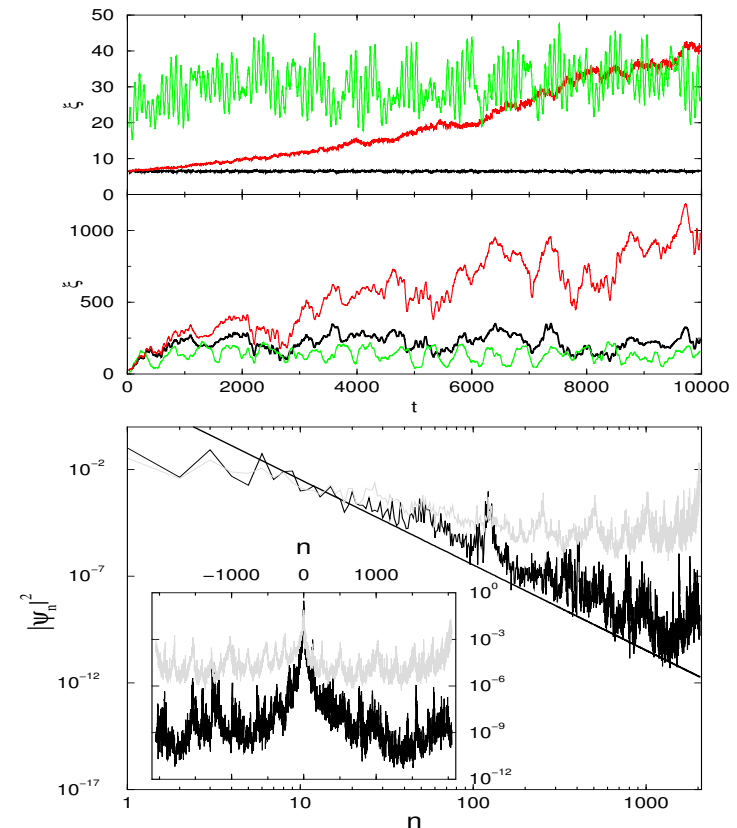
Density plot of the $|U_{n,n'}|^2$. Top: $k = 100$ (left), $k = 1000$ (right); bottom is for $k = 1000$: a doubled resolution of left upper quarter (left), perturbed operator with static errors.

Imperfections

We simulate the gate sequence in the presence of imperfections:

- **Noisy gates:** each gate is perturbed by a random unitary rotation by an angle η , $-\epsilon/2 \leq \eta \leq \epsilon/2$.
- **Static imperfections:** given by the Hamiltonian $H = \sum_l \eta_l \sigma_l^z + \mu_l \sigma_l^x \sigma_{l+1}^x$ ($l = 1, \dots, n_q$). η_l static one-qubit energy shifts, $-\epsilon/2 \leq \eta_l \leq \epsilon/2$, μ_l inter-qubit coupling, $-\mu/2 \leq \mu_l \leq \mu/2$

Effects on IPR ξ and on the wave function ψ_n .



Fidelity time scales

Fidelity: $f(t) = |\langle \psi_\epsilon(t) | \psi(t) \rangle|^2$
 n_g gates per map iteration
 $N_g = n_g t_f$ total number of gates
 $f(t_f) = 0.9$ timescale definition

- Noisy gates:**

$$f(t) \approx \exp(-A\epsilon^2 n_g t)$$

$$t_f = C / (\epsilon^2 n_g)$$

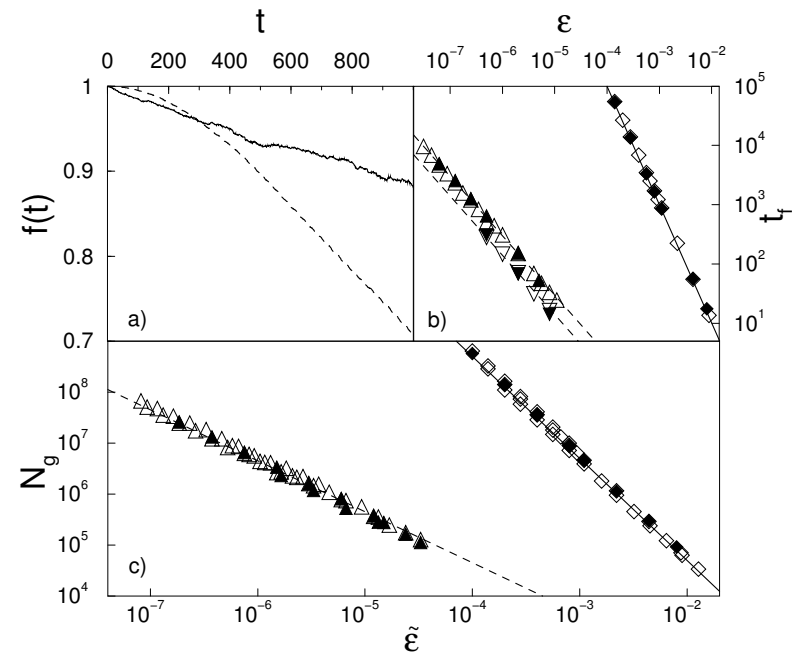
$$N_g = C / (\epsilon^2)$$

- Static imperfections:**

$$f(t) \approx \exp(-n_q (\epsilon n_g t)^2)$$

$$t_f = D / (\epsilon n_g \sqrt{n_q})$$

$$N_g = D / (\epsilon \sqrt{n_q})$$



Panels: a) fidelity scaling; b) t_f vs. ϵ for noisy gates (diamonds), static imperfections (triangles $\mu = 0$, circles $\mu = \epsilon$). c) N_g scalings: $\tilde{\epsilon} = \epsilon$ for noisy gates, $\tilde{\epsilon} = \epsilon \sqrt{n_q}$

Threshold for Fault Tolerant Quantum Computation

Fault Tolerant Quantum Computation (FTQC): Assumptions of **random errors** (corresponding to noisy gates in our simulations)

Accuracy border $p_r = \epsilon_r^2 \sim 10^{-4} \rightarrow$ fidelity is close to 1 up to $N_g \sim C/\epsilon_r^2$ gates.

Static Imperfections: new threshold $\epsilon_s \sim D\epsilon_r^2/(Cn_q^{1/2})$

for $n_q = 10$, D and C from our numerical data we obtain $p_s = \epsilon_s^2 \sim 10^{-9}$.

New techniques to correct static errors: spin echo techniques ????

References:

- A. Fijaney and C. Williams, *Lecture Notes in Computer Science* **1509**, 10 (Springer, 1998);
P.Hoyer, *quant-ph/9702028* (1997) (QWT); A.Steane, *quant-ph/0207119* (2002) (FTQC);
I.Daubechies, *Ten Lectures on wavelets*, CBMS-NSF Series in App. Math., (SIAM, Phil., 1999).

The (classical and quantum) sawtooth map

Time-dependent Hamiltonians with periodicity on q and p . The discretised dynamics, parametrised by K and L , is a “kick” followed by a free evolution:

$$\bar{q} = q + \bar{p} \bmod 2\pi \quad \bar{p} = p - K \frac{dV}{dq} \bmod 2\pi L \quad V(q) = \frac{q^2}{2} (\text{sawtooth})$$

In the quantum case one introduces the number of levels N (with $\hbar = 2\pi L/N$). The Floquet operator (evolution operator corresponding to one iteration of the map) is a product of two terms, which are diagonal respectively in \hat{p} and \hat{q} .

$$U_F = e^{-i\hat{p}^2/2\hbar} e^{-iK V(\hat{q})/\hbar} = \exp \left[-i\frac{\pi L}{N} \hat{n}_p^2 \right] \cdot \exp \left[-i\frac{K}{L} \left(\frac{2\pi}{N} \right)^{\alpha-1} \mathcal{P}_\alpha(\hat{n}_q) \right]$$

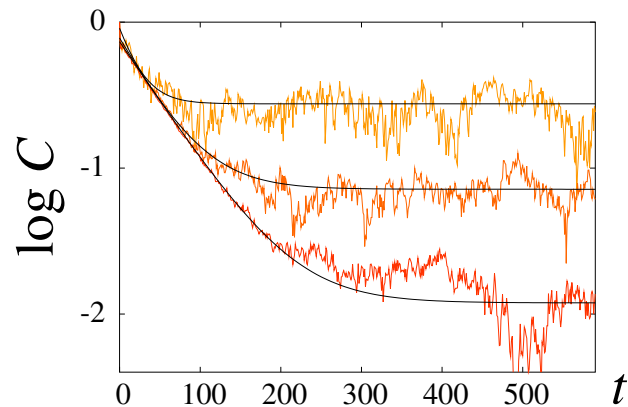
Complexity: $n_g \sim n_q^\alpha \rightarrow n_q^2$. High level primitives are broken down into one or two qubit gates. Algorithm implemented using a quantum language developed in [7], numerical experiments performed up to $n_q \sim 20$ qubits.

Characterisation of entanglement

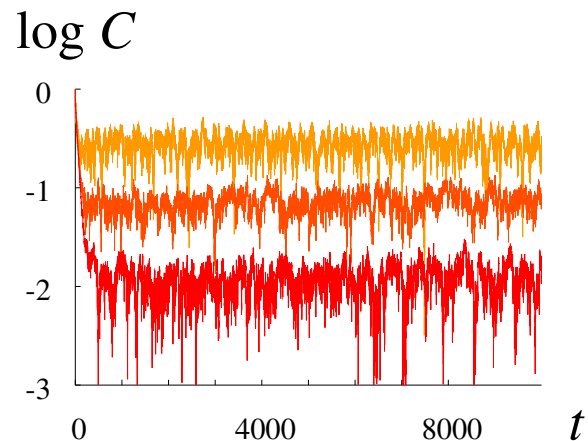
We have chosen to study the evolution of the entanglement of formation of the two most significant qubits in the quantum computer memory while the quantum sawtooth map algorithm is running, using the “concurrence” C . The concurrence depends on the reduced density matrix ρ of the two qubits. If one defines $\tilde{\rho} = (\sigma_y \otimes \sigma_y)\rho^*(\sigma_y \otimes \sigma_y)$, then C is $\max\{0, \lambda_1 - \lambda_2 - \lambda_3 - \lambda_4\}$ where the λ_i are the square roots of the eigenvalues, in decreasing value order, of $\sqrt{\tilde{\rho}\rho}\sqrt{\tilde{\rho}}$ [see Wootters, Phys. Rev. Lett. **80**, 2245 (1998)]. The initial state we use is $|\psi\rangle \propto (|00\rangle + |11\rangle) \otimes |\phi\rangle$, for which $C = 1$, and L is always a multiple of 4.

This quantity does not account for the overall entanglement of the quantum memory, but it has been proven to be linked to interesting physical properties (like quantum phase transitions), and its degradation due to “errors” in the computation should be correlated to the powerfulness of the computation.

Behaviour of the concurrence for an ideal computer

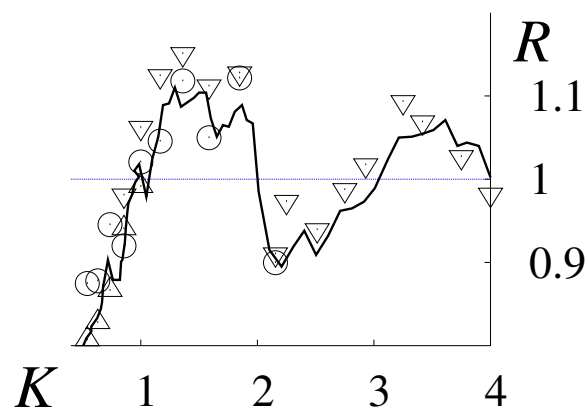
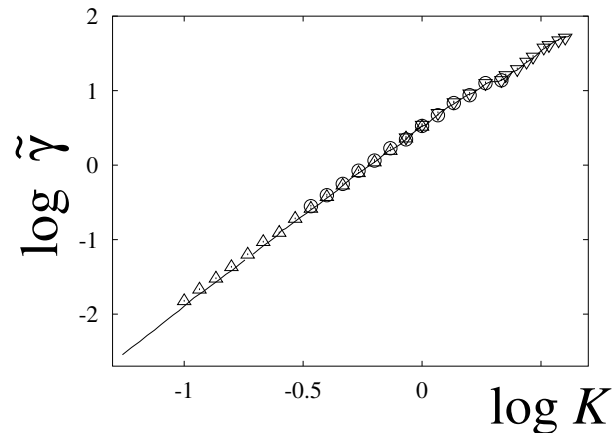


Initial evolution of the concurrence for the sawtooth map at $K = 0.5$, $L = 4$ and $n_q = 8, 12, 16$ (curves from top to bottom respectively). The smooth curves show the fit $C(t) = A \exp(-\gamma t) + \overline{C}$ of the relaxation to the asymptotic value \overline{C} .



Behaviour of $C(t)$ on a larger time scale, showing the asymptotic regime. The initial state is $(|00\rangle + |11\rangle)|\phi\rangle/\sqrt{2}$ where $|\phi\rangle$ is the uniform superposition of all but the two most significant qubits.

Classical diffusion and concurrence decay

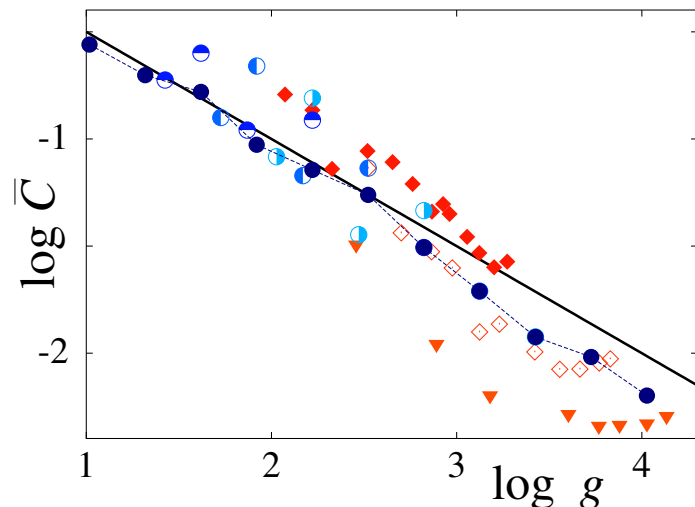


Dependence of the rescaled rate of the concurrence decay, $\tilde{\gamma} = 2\gamma L^2 = (\gamma/\gamma_c)D_0(K)$, on the chaos parameter K for $n_q = 19, L = 16$ (triangles down); $n_q = 18, L = 8$ (circles) and $n_q = 17, L = 4$ (triangles up). The solid curve gives the values of the diffusion rate $D_0(K)$.

This picture shows the data on a larger scale with $R = \tilde{\gamma}/D_{ql}$ (symbols) and $R = D_0(K)/D_{ql}$. It is evident that $\tilde{\gamma}$ follows not only the general trend of D_0 but also its oscillations, showing that γ is almost exactly the classical relaxation rate $\gamma_c = D_0(K)/(2L^2)$.

Numerical results on the residual value of the concurrence

This picture shows the dependence of the residual value of the concurrence

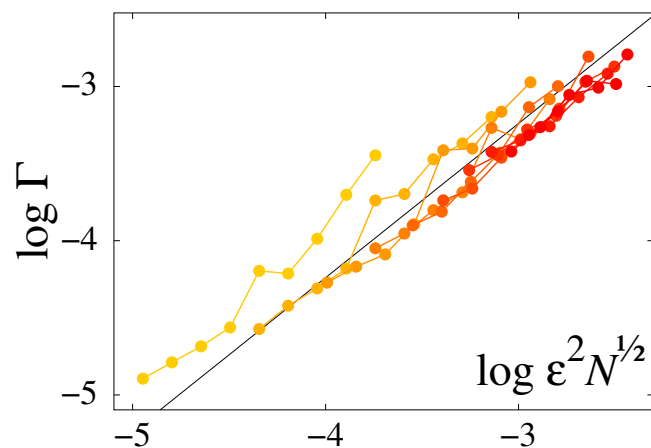


\bar{C} versus the conductance $g = ND_0(K)/L^2$: half filled circles show the dependence on $L = 4, 8, 12, 16, 20$ for $K = 0.5$ and $n_q = 14, 15, 16$; diamonds and triangles show the variation with K for $n_q = 14, L = 16$; $n_q = 15, L = 8$ and $n_q = 16, L = 4$. The filled circles connected by dashed lines show the dependence on N for $K = 0.5, L = 4$.

The solid line marks the slope $1/\sqrt{g}$. We attribute the presence of strong fluctuations to the fact that the value \bar{C} is averaged only over the time but there is no averaging over the parameters. Thus, from the point of view of disordered systems \bar{C} represents only one value for one realisation of disorder.

Concurrence decay induced by noisy gates

This picture illustrates the dependence of the decay rate on the error intensity and the number of qubits. The straight line shows the averaged behaviour $\Gamma = 0.58\epsilon^2\sqrt{N}$. Quite naturally we find that $\Gamma \propto \epsilon^2$ [see, for instance, • Phys. Rev. A, **66**, 054301 (2002)].



This scaling becomes better and better for large ϵ values where Γ is larger. However, more surprisingly there is an exponential growth of $\Gamma \propto \sqrt{N}$. This result is very different from those obtained in other papers [see • and Phys. Rev. Lett. **87**, 227901 (2001)], where the

time scale for the fidelity and the decoherence rate for tunnelling oscillations varied polynomially with n . A possible explanation is that the eigenstates are exponentially sensitive to imperfections due to the chaotic structure of the wave functions [see e.g. Eur. Phys. J. D **20**, 293 (2002)].

Quantum phase space distributions

Quantum algorithm simulating the **quantum kicked rotator** model, a system displaying quantum chaos and dynamical localization; phase space= cylinder (θ = phase, n = momentum). Classical dynamics controlled by $K = kT$. **Global chaos** sets in for $K > K_g = 0.9716\dots$

$$\bar{\psi} = \hat{U}\psi = e^{-ik \cos \hat{\theta}} e^{-iT\hat{n}^2/2}\psi$$

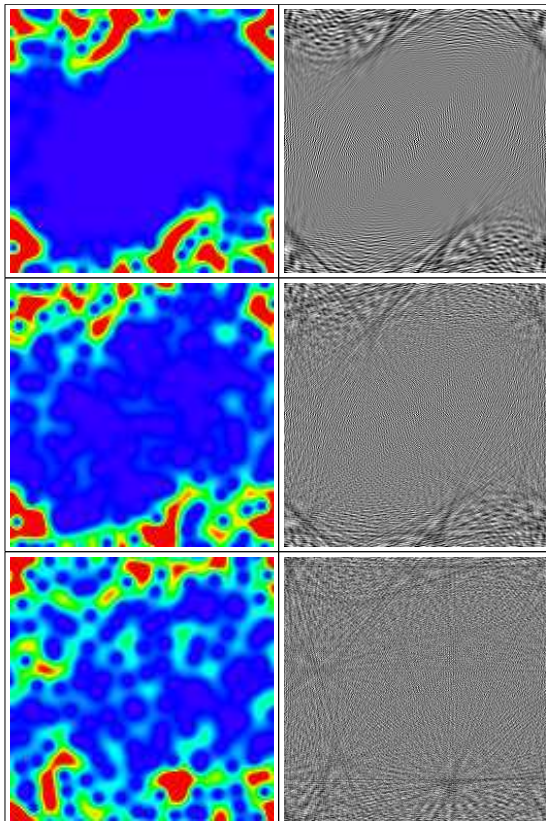
Wigner distribution in phase space: \rightarrow **real but positive or negative**

$$W(\theta, n) = \sum_{m=0}^{N-1} \frac{e^{-\frac{2i\pi}{N}n(m-\Theta/2)}}{2N} \psi(\Theta - m)^* \psi(m), \text{ with } \Theta = \frac{N\theta}{2\pi}.$$

Husimi distribution: $W(\theta, n)$ Gaussian-smoothed over cells of size $\hbar \rightarrow$ **real non negative**

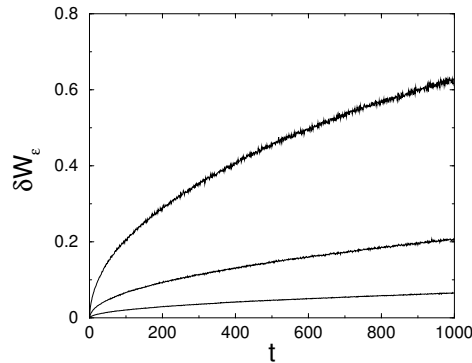
Both functions permit **direct comparison** with **classical phase space densities**

Wigner and Husimi distributions with imperfections

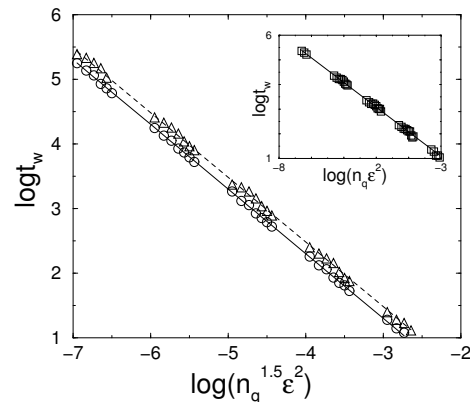


Plot of **Husimi** (left) and **Wigner** (right) distributions for the quantum kicked rotator simulated on a quantum computer at $t = 10^3$ for $K = 1.3 > K_g$, $T = 2\pi/N$, $N = 2^{n_q}$ and number of qubits $n_q = 7$. Initial state is $|\Psi_0\rangle = |n_0\rangle$, with $n_0 = 1$. Top: **amplitude of noise** in gates is $\epsilon = 0$; middle: $\epsilon = 0.002$; bottom: $\epsilon = 0.004$. Left: color represents intensity level from blue (minimal) to red (maximal). Right: grayness represents amplitude of the Wigner function, from white (minimal negative value) to black (maximal positive value).

Stability of individual values of Wigner function

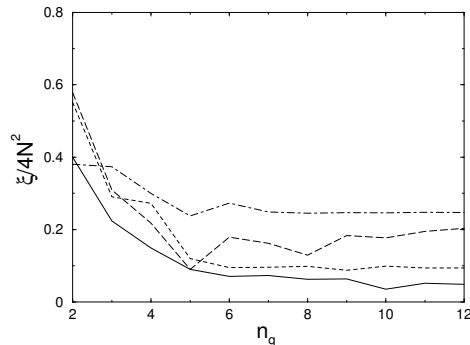


Relative error on the Wigner function $\delta W_\epsilon = \langle |W - W_\epsilon| \rangle / \langle |W| \rangle$ as a function of time for $K = K_g$, $T = 2\pi/N$, $N = 2^{n_q}$ and $n_q = 10$. From bottom to top quantum noise is $\epsilon = 10^{-4}$, $\epsilon = 10^{-3.5}$, $\epsilon = 10^{-3}$. W is averaged over $2N$ values in the chaotic zone.

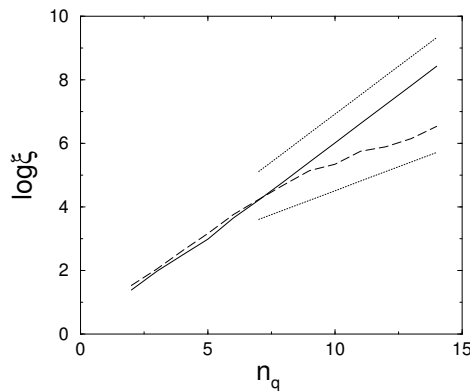


Time scale t_W such that $\delta W_\epsilon(t_W) = 1/2$ vs system parameters for $5 \leq n_q \leq 11$. Here $K = K_g$, $T = 2\pi/N$. W is averaged in the **chaotic** (\circ) or **integrable** (\triangle) zones. Straight lines: theoretical formula $t_W \approx C_W / (n_q^\alpha \epsilon^2)$, with $\alpha = 1.5$, $C_W = 0.02$ (full line) or $C_W = 0.03$ (dashed line). Inset: same for $T = 0.5$ and $K = 5$ and $5 \leq n_q \leq 14$. W is averaged in the **localized** zone. Full line: theoretical formula with $\alpha = 1$, $C_W = 0.012$.

Statistical properties of individual values of Wigner function



Inverse participation ratio $\xi = 1/(\mathbf{N}^2 \sum \mathbf{W}_i^4)$ of the **Wigner function** vs n_q at $t = 10^3$ and $\epsilon = 0$ for $T = 2\pi/N$, $N = 2^{n_q}$ and $K = 0.5$ (full curve), $K = 0.9$ (dashed curve), $K = 1.3$ (long-dashed curve), $K = 2.0$ (dot-dashed curve).



ξ vs n_q at $t = 10^3$ and $\epsilon = 0$ for $T = 2\pi/N$, $N = 2^{n_q}$ and $K = 2$ (full line), and $T = 0.5$ and $K = 5$ (dashed line). Dotted lines show $\xi \propto \mathbf{N}^2$ (i.e. $\mathbf{W}_i \propto 1/\mathbf{N}^{3/2}$) (**non-localized** regime) and $\xi \propto \mathbf{N}$ (i.e. $\mathbf{W}_i \propto 1/\mathbf{N}$) (**localized** regime).

Strong superadditivity of the entanglement of formation follows from its additivity

Entanglement of formation

Entanglement of two subsystems A and B in a pure state:
 $E(\psi) = S(\text{Tr}_B(|\psi\rangle\langle\psi|)) = S(\text{Tr}_A(|\psi\rangle\langle\psi|))$,
where S is the von Neumann entropy: $S(\rho) = -\text{Tr}\rho \log_2 \rho$.
For mixed states: the *entanglement of formation* (EoF):
 $E_F(\rho) = \min_{\{p_i, \psi_i\}} \sum_i p_i E(\psi_i)$,
with $\rho = \sum_i p_i |\psi_i\rangle\langle\psi_i|$ (C.H. Bennett et al. (1996)).

Additivity

Let us consider two separate systems 1 and 2 (each is a bipartite system with the parts $1A$, $1B$ and $2A$, $2B$ respectively, we always consider entanglement between A and B). What is the EoF of the state $\rho_1 \otimes \rho_2$ of the composite system? It has been conjectured that it is the sum of the EoFs of the parts 1 and 2 (the EoF is *additive*):

$$E_F(\rho_1 \otimes \rho_2) \stackrel{?}{=} E_F(\rho_1) + E_F(\rho_2).$$

This is trivially true for pure states. There are proofs for particular classes of states (G. Vidal et al. (2002)).

Strong superadditivity

Within the same setting, it is natural to compare the EoF of a system with the sum of the EoF's of its subsystems. It has been conjectured (K.G.H. Vollbrecht and R.F. Werner (2001)) that the former is not less than the latter:

$$E_F(\rho) \stackrel{?}{\geq} E_F(\text{Tr}_2\rho) + E_F(\text{Tr}_1\rho).$$

This property is called **strong superadditivity**. It is sufficient to prove this conjecture for pure states. The strong superadditivity **implies** both the additivity of the EoF and that of the Holevo classical channel capacity (K. Matsumoto et al. (2002)).

Equivalence of the conjectures

We show that, conversely, the additivity of the EoF **implies** the strong superadditivity, that is **the two conjectures are equivalent** (see [5] for the details). We used the methods of convex analysis, introduced in this context by K.M.R. Audenaert and S.L. Braunstein (quant-ph/0303045), most notably the notion of the conjugated function. We use also some properties of optimal decompositions of density matrices which are known from the work of F. Benatti and H. Narnhofer (2001).

P.W. Shor (quant-ph/0305035) has proved that the additivity of the EoF, the strong superadditivity of the EoF, the additivity of the Holevo classical channel capacity and the additivity of the minimal output entropy conjectures are all equivalent.



The HAL Quantum Speech

- [original HAL speech](#)
- [measurements in frequency domain](#)
- [10 measurements per frame](#)
- measurements in frequency domain with quantum errors (amplitude of gate errors 0.05)
- [10 measurements per frame](#)
- measurements in time domain
- [10 measurements per frame](#)
- quantum sound of coarse grained Wigner function
- [10 measurements per frame](#)
- [download all sound files \(2 Mhz\)](#)

"Good afternoon, gentlemen. I am a HAL 9000 computer. I became operational at the H. A. L. lab in Urbana, Illinois on the 12th of January"

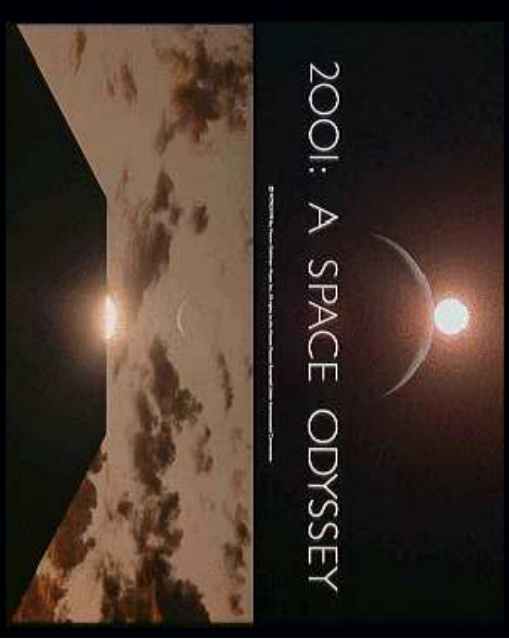
This sound is encoded on an 18 qubit quantum computer and it is recovered with a finite number of quantum measurements performed in time or frequency domain (MP3 like) in presence of gate imperfections.

We can also listen the sound of a complex quantum wavefunction generated by an efficient quantum algorithm (14 qubits).

Quantum computations are done on Quantum I simulated numerically on Pentium IV

The paper is at <http://xxx.lanl.gov>

The original HAL speech and 2001 A Space odyssey picture are taken from <http://www.palantir.net/2001/>



Papers from the QUANTWARE group

(from August 2002 to August 2003)

- [1] G.Benenti, G.Casati, S.Montangero and D.L.Shepelyansky, "Dynamical localization simulated on a few qubits quantum computer", Phys. Rev. A **67**, 052312 (2003), quant-ph/0210052.
- [2] B.Levi, B.Georgeot and D.L.Shepelyansky, "Quantum computing of quantum chaos in the kicked rotator model", Phys. Rev. E **67**, 046220 (2003), quant-ph/0210154.
- [3] S.Bettelli and D.L.Shepelyansky, "Entanglement versus relaxation and decoherence in a quantum algorithm for quantum chaos", Phys. Rev. A **67**, 054303 (2003), quant-ph/0301086.
- [4] M.Terraneo and D.L.Shepelyansky, "Imperfection effects for multiple applications of the quantum wavelet transform", Phys. Rev. Lett. **90**, 257902 (2003), quant-ph/0303043.
- [5] A.A.Pomeransky, "Strong superadditivity of the entanglement of formation follows from its additivity", (to appear in Phys. Rev. A) quant-ph/0305056.
- [6] A.A.Pomeransky and D.L.Shepelyansky, "Quantum computation of the Anderson transition in presence of imperfections", submitted to Phys. Rev. Lett., preprint quant-ph/0306203.
- [7] S.Bettelli, T.Calarco and L.Serafini, "Toward an architecture for quantum programming", Eur. Phys. J. D **25**, 181-200 (2003), cs.PL/0103009
- [8] J.W.Lee, A.D.Chepelianskii and D.L.Shepelyansky, "Treatment of sound on quantum computers", quant-ph/0309018.